BIOLOGY OF REPRODUCTION **81,** 177–187 (2009)
Published online before print 1 April 2009.
DOI 10.1095/biolreprod.109.076299

Histological and Stereological Evaluation of Zebrafish (*Danio rerio*) Spermatogenesis with an Emphasis on Spermatogonial Generations[1]

Marcelo C. Leal,[5,6] Edson R. Cardoso,[5] Rafael H. Nóbrega,[5,6] Sergio R. Batlouni,[5] Jan Bogerd,[6] Luiz R. França,[2,4,5] and Rüdiger W. Schulz[3,4,6,7]

Laboratory of Cellular Biology,[5] Department of Morphology, Institute of Biological Sciences, Federal University of Minas Gerais, Belo Horizonte, Brazil
Division of Endocrinology & Metabolism,[6] Biology Department, Science Faculty, Utrecht University, Utrecht, The Netherlands
Reproduction and Growth Research Group,[7] Institute of Marine Research, Bergen, Norway

ABSTRACT

The zebrafish has become an important vertebrate model for basic and biomedical research, including the research field of the biology of reproduction. However, very few morphological and stereological data are available regarding zebrafish testis structure and spermatogenesis. In this careful histomorphometric evaluation of the testis, we studied spermatogonial cells using molecular markers, determined the combined duration of meiotic and spermiogenic phases, and examined the formation of the Sertoli cell barrier (tight junctions). We found at least nine spermatogonial generations and propose a morphology-based nomenclature for spermatogonial generations that is compatible with the one used in higher vertebrates. The number of germ cells per cyst increased dramatically (1 to ~1360 cells) from undifferentiated spermatogonia type A to early spermatids. The combined duration of meiotic and spermiogenic phases is approximately 6 days, one of the shorter periods among the teleost fish investigated to date. The number of Sertoli cells per cyst increased 9-fold during the maturational cycle of spermatogenic cysts and stabilized in the meiotic phase at a ratio of approximately 100 early spermatids per Sertoli cell (Sertoli cell efficiency). Similarly to mammals, Sertoli cell proliferation ceased in the meiotic phase, coinciding with the formation of tight junctions between Sertoli cells. Hence, the events taking place during puberty in the germinal epithelium of mammals seem to recapitulate the "life history" of each individual spermatogenic cyst in zebrafish.

Leydig cells, Sertoli cells, spermatogenesis, teleost fish, testis

INTRODUCTION

The zebrafish (*Danio rerio*; family Cyprinidae, order Cypriniformes) is a small freshwater teleost fish (~5 cm in length) originally from Central Asia [1]. Easy handling, high number of progeny, transparent embryos, and forward and reverse genetics approaches have contributed to the importance of this model species in basic and biomedical research; reproductive physiology [2], integrative physiology in general [3], and more applied research fields, such as ecotoxicology [4] or aquaculture [5], increasingly make use of the zebrafish model.

Spermatogenesis is a complex and highly coordinated process by which diploid spermatogonia produce millions of spermatozoa daily [6]. This process is fueled by spermatogonial stem cells, which have the potential for both self-renewal and for differentiating into spermatogonia committed to sperm development [7–9]. In fish, as in other anamniote vertebrates, spermatogenesis occurs in cysts that are formed when a single spermatogonium is completely surrounded by the cytoplasmic projections of one or two Sertoli cells [10]. As in all animals, the cells resulting from differentiating mitotic divisions of single spermatogonia remain interconnected by cytoplasmic bridges that synchronize developmental processes among the members of the same germ cell clone [11, 12]. Thus, in this cystic type of spermatogenesis, a given Sertoli cell is in contact with only one germ cell clone. This is the main difference in relation to noncystic spermatogenesis, as occurs in amniote vertebrates (reptiles, birds, and mammals), where several clones at different stages of development are distributed along basal, lateral, and adluminal surfaces of a Sertoli cell [6, 13, 14]. Apart from the cystic arrangement, the spermatogenic process in teleost fish is very similar to that of mammals [15].

With regard to the biology of male reproduction, zebrafish were studied to assess the effects of endocrine disruptors [2, 16] or the production of reproductive pheromones [17]. However, few quantitative data are available regarding the basic aspects of testis morphology and spermatogenesis in zebrafish. Histological and stereological investigations are adequate approaches to a better understanding of the spermatogenic process and testis function in fish [18, 19]. Such an evaluation allows the determination of the dynamics in the numbers of germ cells and Sertoli cells for each type of spermatogenic cyst, and it provides information on the number of spermatogonial generations, on the magnitude of germ cell loss occurring during spermatogenesis, and on Sertoli cell efficiency.

Our long-term aim is to further our understanding of the regulation of spermatogenesis. We hypothesize that in the cystic mode of spermatogenesis, Sertoli cell functions related to supporting a given stage of spermatogenesis can be studied undisturbed by germ cells in other stages of development, in contrast to noncystic spermatogenesis, where several germ cell clones are in contact with a given Sertoli cell. A basis required for such studies, as well as for other fields, like reproductive toxicology, is a thorough description of zebrafish spermatogenesis, including quantitative data that allow a better

[1]Supported by the Brazilian Foundations FAPEMIG (Fundação de Amparo à Resquisa do Estado de Minas Gerais), CNPq (Conselho Nacional de Desenvolvimento Cientifico e Tecnológico), CAPES (Coordenação de Aperfciçoamento de Pessoal de Nível Superior), and Utrecht University.
[2]Correspondence: FAX: 55 31 34092780; e-mail: lrfranca@icb.ufmg.br
[3]Correspondence: FAX: 31 30 2532837; e-mail: r.w.schulz@uu.nl
[4] These authors contributed equally to this work.

Received: 19 January 2009.
First decision: 18 February 2009.
Accepted: 27 March 2009.

eISSN: 1259-7268 http://www.biolreprod.org
ISSN: 0006-3363

understanding of spermatogenesis. Such data have not yet been published, and the main objectives of the present study were to perform a comprehensive stereological study of the different types of spermatogenic cysts (the number of germ cells and Sertoli cells per spermatogonial, spermatocyte, and spermatid cyst). Although the different stages of meiosis and spermiogenesis are relatively easy to differentiate, the successive spermatogonial generations are not. Therefore, we devoted particular attention to the mitotic phase of spermatogenesis, propose a nomenclature for the different spermatogonial generations, and have started with a molecular characterization of the spermatogonia. Based on these data, we are able to estimate the number of spermatogonial generations, the magnitude of germ cell loss, and Sertoli cell number and efficiency. We also determined the duration of the combined meiotic and spermiogenic phases at 27°C through the incorporation of 5′bromo-2′-deoxyuridine (BrdU). Finally, the permeability of the Sertoli cell barrier was assessed during the spermatogenic phases by using an electron-dense tracer, lanthanum nitrate.

MATERIALS AND METHODS

Animals, Sampling, Biometry, and Testis Structure

Thirty sexually mature zebrafish—outbred animals and Tübingen AB strain (TABs)—were used for histology and stereology (TABs), analysis of the duration of spermatogenesis (TABs), and Sertoli cell barrier analysis (outbred). The animals were anesthetized and weighed, and the testis was dissected out, weighed, and fixed by immersion (see below). The gonadosomatic index (GSI) was obtained by the formula GSI = (testes weight/body weight) × 100. All procedures used followed approved guidelines for the ethical treatment of animals and national laws. Experimental protocols were submitted to, and approved by, the Utrecht University and Federal University of Minas Gerais (CETEA) committees for animal experimentation and care.

Testis Stereology

For histological and stereological analysis, testes were fixed in 4% buffered (PBS) glutaraldehyde at 4°C overnight. The tissue was dehydrated and embedded in 2-hydroxyethyl methacrylate. In a pilot study, we determined the nuclear diameter of the different germ cell types to determine the section thickness that avoids counting the same nucleus twice, using the procedure described previously [20]. According to these results, testes were serially sectioned at 2 and 3 μm thickness; histological sections were stained with 1% toluidine blue.

The total number of germ cells and Sertoli cells per spermatogonial, spermatocyte, and spermatid cyst was counted on serial sections using a total of 13 zebrafish. This evaluation was performed after selecting cysts entirely encompassed by serial sections. At least five cysts were analyzed for each germ cell type in each fish. The Sertoli cell efficiency was estimated from the ratio of germ cells:Sertoli cells for each cyst type.

For a high-resolution light microscopy analysis of the spermatogonial compartment and to differentiate morphologically the spermatogonial generations, small fragments of zebrafish testes (n = 5) were fixed by immersion in 5% glutaraldehyde in 0.05 M sodium cacodylate buffer (pH 7.2–7.4) for at least 24 h. After fixation, the material was rinsed three times in the same buffer, postfixed in osmium-ferrocyanide, dehydrated, embedded in araldite, sectioned for light microscopy (1 μm thick), and stained with toluidine blue.

The individual Leydig and germ cell volumes (μm^3) were obtained from the nuclear volume and the proportion (%) between nucleus and cytoplasm of each cell type evaluated, which were determined as described previously [20].

Germ cell loss (apoptosis) was analyzed qualitatively and quantitatively and was expressed as a percentage of apoptotic cells per cyst. These apoptotic cells were morphologically characterized as darker-stained cells, as is typical in this condition for cells embedded in plastic and stained with toluidine blue [19].

Immunocytochemical and In Situ Hybridization Experiments

Testis tissue from adult males (outbred or TABs) was fixed in 4% paraformaldehyde in PBS overnight at 4°C. For immunocytochemistry, the tissue was rinsed briefly in PBS before being immersed in PBS containing 20% (w/v) sucrose for 1 day at 4°C. Tissue was then frozen in Neg50 (Richard-Allan Scientific, Kalamazoo, MI). Cryosections (10 μm thick) were used to detect Vasa [21] or Piwil1 (also known as Ziwi) [22] protein using previously described antisera raised in rabbit.

Rabbit anti-Vasa was used at a dilution of 1:200 and incubated overnight at room temperature before incubation with a goat anti-rabbit antiserum labeled with fluorescein isothiocyanate (FITC; 1:200; A11008; Invitrogen, Carlsbad, CA) for 90 min at room temperature. The buffer also contained 1 μg/ml propidium iodide to label DNA. The sections were analyzed with a confocal laser scanning microscope using 488 and 536 nm as excitation wavelengths for FITC and propidium iodide, respectively. Detection of Piwil1 protein and staining of DNA by 4′,6′-diamidino-2-phenylindole were done as described by Houwing et al. [22].

For in situ hybridization, paraformaldehyde-fixed tissue was dehydrated and embedded in paraffin according to conventional techniques. Sections of 5 μm thickness were used for the detection of mRNA encoding proliferating cell nuclear antigen (pcna), a protein involved in DNA synthesis and repair [23] and shown to be predominantly expressed in rapidly proliferating spermatogonia in Japanese eel [24]. The zebrafish *pcna* mRNA sequence (http://www.ncbi.nlm.nih.gov/entrez/viewer.fcgi?db=nuccore&id=18859222) was used to design specific primers. A zebrafish *pcna* PCR product (634 bp) was generated using primers 1039 and 1040 (Supplemental Table S1 available online at www.biolreprod.org) and zebrafish testis cDNA as template, and it was gel purified and served as template for digoxigenin (DIG)-labeled cRNA probe synthesis by in vitro transcription. For cRNA synthesis, 300 ng of PCR product was incubated at 37°C for 2.5 h in a 20-μl reaction volume containing 4 μl of 5× T3/T7 RNA buffer (Invitrogen), 2 μl of 0.1 M dithiothreitol, 1 μl (29.7 U/μl) of RNAguard RNase inhibitor (GE Healthcare, Fairfield, CT), 2 μl of 10× DIG RNA labeling mix (Roche, Mannheim, Germany), and either 2 μl (50 U/μl) of T3 RNA polymerase (for sense probe; Epicentre, Madison, WI) or 2 μl (50 U/μl) of T7 RNA polymerase (for antisense probe; Epicentre).

Duration of Spermatogenesis (Meiotic and Spermiogenic Phases)

To estimate the combined duration of meiotic and spermiogenic phases at 27°C, 16 animals (TABs) were exposed to BrdU dissolved in water (3 mg/ml) for approximately 15 h. The animals (n = 2 per time point investigated) were sampled at 1 h and at 1, 2, 3, 4, 5, 6, and 7 days after the exposure was terminated.

BrdU incorporation was detected following a protocol modified from Van de Kant and de Rooij [25]. Zebrafish testes were fixed for 5 h at room temperature in freshly prepared methacarn (60% [v/v] absolute ethanol, 30% chloroform, and 10% glacial acetic acid) and embedded in Technovit 7100 (Heraeus Kulzer, Wehrheim, Germany). Five-micrometer-thick sections were subjected to antigen retrieval (1% [v/v] periodic acid in water at 60°C for 30 min) and peroxidase blocking (1% [v/v] H_2O_2 in PBS for 10 min). Thereafter, slides were incubated at room temperature for 1 h with mouse anti-BrdU (1:80 [BD Biosciences, San Jose, CA] diluted in PBS containing 1% [w/v] bovine serum albumin [BSA; Sigma-Aldrich, St. Louis, MO]), and then for an additional hour with biotinylated horse anti-mouse (1:100 [Vector Laboratories, Burlingame, CA] diluted in PBS containing 1% [w/v] BSA). Revelation of immunostaining was done using avidin-biotin complex incubation for 1 h (Vector Laboratories) followed by diaminobenzidine (Dako, Glostrup, Denmark) substrate development for 20 sec. Nuclei were counterstained with hematoxylin Gill no. 3 (Sigma-Aldrich) for 30 sec. For a negative control, the primary antibody (mouse anti-BrdU) was replaced with the same concentration of normal mouse immunoglobulin G (BD Biosciences).

Sertoli Cell Barrier

To investigate the presence and timing of the formation of the Sertoli cell barrier (tight junctions between Sertoli cells) during spermatogenesis, lanthanum nitrate ($La(NO_3)_3$) was prepared by slowly adding drops of 0.01 N NaOH to 2% $La(NO_3)_3$ (Vetec, Rio de Janeiro, Brazil) until the solution reached pH 7.8. This opalescent solution was mixed with an equal volume of cacodylate-buffered glutaraldehyde to make a fixative containing 1% lanthanum and 2% glutaraldehyde in 0.1 M cacodylate at pH 7.8 or 7.3.

The testes from outbred animals were prefixed for 2 min in the fixative containing lanthanum, and then small pieces (2–3 mm^3) were fixed by immersion in the same fixative for 5 h at room temperature. The material was rinsed overnight in the same lanthanum solution without glutaraldehyde at 4°C (pH 7.8 or 7.3 according to the fixative pH). The samples were postfixed for 8 h in 1% OsO_4 in 0.1 M cacodylate buffer containing 1% lanthanum at pH 7.8 or 7.3 (according to the fixative pH). After overnight staining in 0.5% aqueous uranyl acetate, the material was dehydrated in alcohol, embedded in araldite, and documented using a JEOL 100 CX-II transmission electron microscope (80 kV).

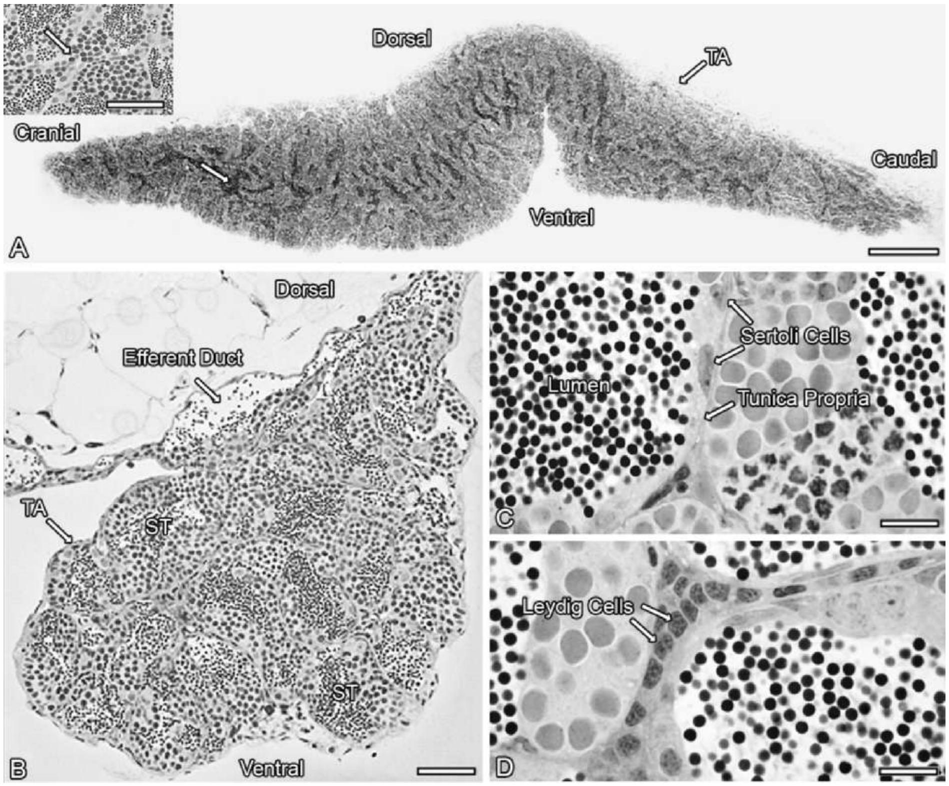

FIG. 1. **A**) Longitudinal section of a zebrafish testis showing the dorsal-ventral and caudal-cranial axis. The tunica albuginea (TA) externally surrounds the testis. The seminiferous tubules sometimes show an anastomosing pattern (arrow in **A** and the inset). **B**) Cross-section of zebrafish testis showing the tunica albuginea (TA), the efferent duct, and seminiferous tubules (ST). **C**) Tubular compartment of the testis showing tunica propria surrounding the seminiferous tubule, Sertoli cells often in the basal region of spermatogenic cysts, and lumen containing spermatozoa. **D**) Intertubular compartment showing a cluster of Leydig cells. Bars = 400 μm (**A**), 50 μm (inset and **B**), and 10 μm (**C** and **D**).

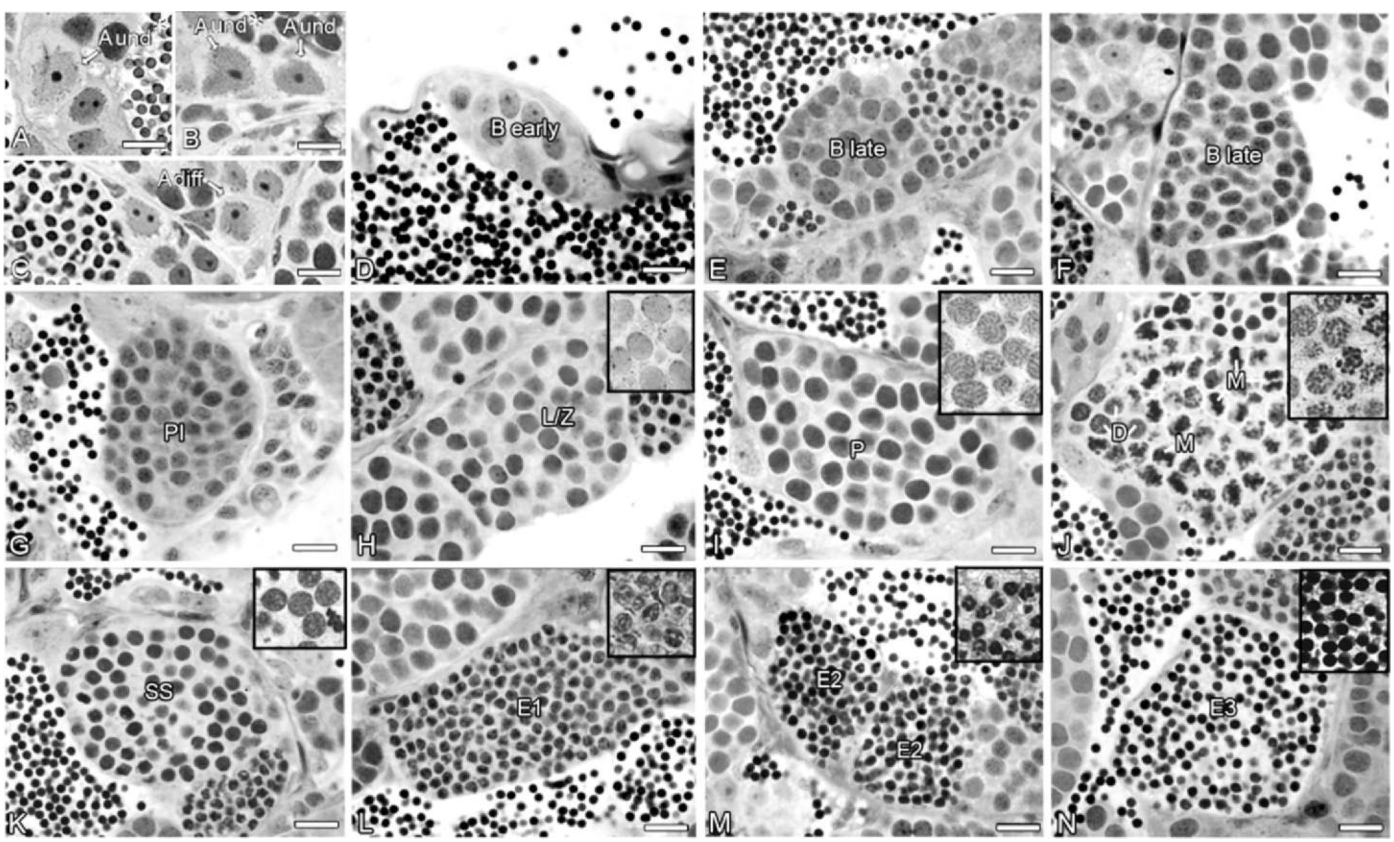

FIG. 2. Different germ cell cysts observed during the spermatogenic process in zebrafish from a type A undifferentiated* spermatogonium to spermatids before spermiation. **A**) The most undifferentiated type A spermatogonium (A_{und}*; probable stem cell; refer to Fig. 3 for a more detailed account on spermatogonia). **B**) Type A undifferentiated spermatogonium (A_{und}*) and type A undifferentiated spermatogonium (A_{und}; possibly limited stem cell capacity). **C**) Type A differentiated spermatogonia (A_{diff}). **D**) Early type B spermatogonia (B_{early}). **E** and **F**) Late type B spermatogonia (B_{late}). **G**–**J**) Primary spermatocytes in preleptotene (Pl), in the transition of leptotene to zygotene (L/Z), pachytene (P), diplotene (D), and meiotic figures from the first meiotic division (M). **K**) Secondary spermatocytes (SS). **L**–**N**) Spermatids at initial (E1), intermediate (E2), and final (E3) steps of development. Bars = 10 μm (or 5 μm for the insets in **H**–**N**).

TABLE 1. Stereology of the different germ cell cysts in zebrafish (n = 8; mean ± SEM).

			Germ cells					
Cyst type*	No. of Sertoli cells per cyst	No. of germ cells per cyst†	Nuclear diameter (μm)	Nuclear volume (μm^3)‡	Cytoplasm volume (μm^3)§	Cell volume (μm^3)	Cyst volume (μm^3)¶	No. of germ cells (cyst) per Sertoli cell
SPG_1–A_{und}	1.2 ± 0.1[a]	1.0 ± 0[a]	8.6 ± 0.1[a]	336 ± 16 (0.50)[a]	342 ± 18[a] (0.50)	677 ± 34[a]	677 ± 34[a]	0.8 ± 0.1[a]
SPG_2–$A_{diff}1$	2.1 ± 0.1[b]	2.0 ± 0[b]	6.6 ± 0.1[b]	150 ± 4 (0.51)[b]	147 ± 6[b] (0.49)	297 ± 9[b]	593 ± 18[a]	1.0 ± 0.1[a]
SPG_3–$A_{diff}2$	2.7 ± 0.1[b]	3.7 ± 0[c] [4]	6.0 ± 0.1[c]	112 ± 1 (0.52)[c]	105 ± 3[c] (0.48)	216 ± 4[c]	790 ± 14[a]	1.4 ± 0.1[a]
SPG_4–$A_{diff}3$	3.9 ± 0.2[c]	7.2 ± 0.1[c] [8]	5.7 ± 0.1[d]	99 ± 1 (0.55)[c]	81 ± 3[c,d] (0.45)	180 ± 3[c,d]	1318 ± 24[a]	1.8 ± 0.1[a]
SPG_5–B1	5.1 ± 0.2[d]	14 ± 0.3[c] [16]	5.6 ± 0.1[d]	92 ± 1 (0.58)[c,d]	66 ± 4[d,e] (0.42)	158 ± 5[d,e]	2159 ± 69[a]	2.7 ± 0.1[a]
SPG_6–B2	5.4 ± 0.1[d]	28 ± 1[c] [32]	5.3 ± 0.1[e]	76 ± 1 (0.60)[d,e]	51 ± 2[e,f] (0.40)	128 ± 2[e,f]	3624 ± 90[a]	5.3 ± 0.1[a,b]
SPG_7–B3	6.2 ± 0.1[e]	55 ± 1[c,d] [64]	5.1 ± 0.1[e,f]	71 ± 0.5 (0.61)[d,f]	45 ± 1[e,g] (0.39)	116 ± 2[f,g]	6473 ± 190[a,b]	9 ± 0.3[b,c]
SPG_8–B4	9.3 ± 0.2[f]	113 ± 3[d] [128]	5.0 ± 0.1[f]	64 ± 1 (0.61)[e,f,g]	41 ± 2[e,h] (0.39)	105 ± 2[f,g]	11 949 ± 429[b,c]	12 ± 0.2[c]
SPG_9–B5	11.2 ± 0.4[g]	208 ± 8[e] [256]	4.7 ± 0.1[g]	53 ± 1 (0.64)[f,h]	29 ± 1[f,g,h,i] (0.36)	82 ± 1[f,g,h]	16 945 ± 755[c,d]	19 ± 1.1[d]
Pl	11.9 ± 0.2[h]	423 ± 9[f] [512]	4.4 ± 0.1[h]	45 ± 1 (0.61)[g,h,i]	29 ± 2[f,g,h,j] (0.39)	74 ± 3[g,h,i]	31 325 ± 1283[e]	36 ± 0.8[e]
L/Z	12.0 ± 0.3[g,h]	395 ± 12[f]	5.1 ± 0.1[e,f]	70 ± 1 (0.59)[e,f,h]	48 ± 3[e,i,j] (0.41)	117 ± 4[e,f,g,h,i]	46 087 ± 1163[f]	33 ± 0.6[e,f]
P	12.8 ± 0.2[i]	377 ± 19[f]	6.0 ± 0.1[c]	112 ± 2 (0.60)[c,d]	76 ± 1[d,e] (0.40)	188 ± 2[c,e]	71 585 ± 3602[g]	30 ± 1.5[f]
D	13.0 ± 0.4[i,j]	397 ± 8[f]	5.2 ± 0.1[e,f]	74 ± 2 (0.61)[d,g,h]	48 ± 3[e,i,j] (0.39)	122 ± 4[e,f,g,h]	48 608 ± 1539[f]	31 ± 1.2[e,f]
S	13.8 ± 0.4[j,k,l]	768 ± 26[g] [1024]	3.9 ± 0.1[i]	31 ± 1 (0.59)[i,j]	21 ± 1[g,h,i] (0.41)	52 ± 2[h,i,j]	38 808 ± 1362[h]	56 ± 1.7[g]
E1	14.3 ± 0.4[k]	1353 ± 45[h] [2048]	3.0 ± 0.1[j]	14 ± 0.2 (0.60)[j,k]	9 ± 1[i,j] (0.40)[#]	22 ± 1[j]	29 465 ± 1183[e]	94 ± 2.34[h]
E2	14.1 ± 0.3[k]	1299 ± 23[h,i]	2.5 ± 0.1[k]	8 ± 0.3 (0.61)[k]	5 ± 0.3[i,j] (0.39)	14 ± 1[j]	17 616 ± 773[c,d]	92 ± 2.3[h]
E3	13.1 ± 0.2[i,l]	1262 ± 13[i]	2.1 ± 0.1[l]	5 ± 0.1 (0.60)[k]	3 ± 0.1[i,j] (0.40)	8 ± 0.1[j]	10 771 ± 185[b,c]	96 ± 1.6[h]

* SPG_1–A_{und}, primary spermatogonia; SPG_2–$A_{diff}1$, SPG_3–$A_{diff}2$, SPG_4–$A_{diff}3$, different generations of type A differentiated spermatogonia; SPG_5–B1, SPG_6–B2, different generations of type B early spermatogonia; SPG_7–B3, SPG_8–B4, SPG_9–B5, different generations of type B late spermatogonia; Pl, preleptotene primary spermatocytes; L/Z, leptotene/zygotene primary spermatocytes; P, pachytene spermatocytes; D, diplotene spermatocytes; S, secondary spermatocytes; E1, initial spermatids; E2, intermediate spermatids; E3, final (mature) spermatids.
† Values in brackets indicate the theoretical number of germ cells formed after mitotic and meiotic divisions.
‡ Values in parentheses are the percentage of nucleus in the cell.
§ Values in parentheses are the percentage of cytoplasm in the cell.
¶ Sertoli cells not included.
# Flagellum included.
[a-l] Different superscript letters indicate that mean values differ significantly ($P < 0.05$).

Statistical Analysis

All quantitative data are presented as the mean ± SEM and analyzed via ANOVA (Student-Newman-Keuls test). The analysis was performed using the software STATISTICA 3.11 for Windows (StatSoft Inc., Tulsa, OK). The significance level in comparisons was considered to be $P < 0.05$.

RESULTS

Biometry and Testis Structure

The mean testis weight of zebrafish was 4.7 ± 0.2 mg, resulting in a GSI of 1.0% ± 0.05%. The testes are paired and elongated organs that stretch dorsally through the length of the body cavity and are connected to the dorsal body wall via the mesorchium. The testes join caudally to form a single spermatic duct that terminates on the urogenital papilla. The anastomosing seminiferous tubules (Fig. 1A and inset, arrows) empty dorsally into the main testicular efferent duct (Fig. 1B) that continues caudally as a single spermatic duct. Different types of germ cell cysts (from spermatogonia to spermatids) are distributed along the seminiferous epithelium (Fig. 2 and Supplemental Fig. S1).

Number of Germ Cells and Sertoli Cells per Cyst

All stereological data are presented in Table 1. The total number of Sertoli cells per cyst increased gradually and significantly from type A undifferentiated spermatogonium to pachytene spermatocyte cysts, and it shows a strong trend toward stabilization from diplotene spermatocytes to mature spermatids (Table 1). The number of germ cells per cyst increased geometrically, as expected, from a single type A undifferentiated spermatogonium to early spermatids, showing a reduction of 7% of the expected theoretical number from intermediate to final spermatid cysts (Table 1).

The data obtained for the number of spermatogonia and early spermatocytes per cyst allowed us to estimate that nine generations of spermatogonia are present in zebrafish—one generation of type A undifferentiated spermatogonia (see below for morphological details on two forms of type A undifferentiated spermatogonia that are both found as single germ cells in early cysts), three generations of type A differentiating spermatogonia, and five generations of type B (early: B1–B3; late: B4 and B5) spermatogonia. Because the nuclear morphology among the different generations of type B spermatogonia was very similar, the criteria used to distinguish each generation of this cell type were the decreasing cell size and the increasing number of spermatogonia per cyst. Regarding the Sertoli cell efficiency for spermatids, approximately 100 spermatids were found per Sertoli cell. Considering the theoretical number expected and the number obtained, we can estimate that the total germ cell loss during spermatogenesis was ~38%. Using the deviation from theoretical number of germ cells for each generation, germ cell loss (by apoptosis) occurs in two steps—in the final spermatogonial generation and during the first meiotic prophase (B5 to diplotene), and then during the second meiotic division (secondary spermatocytes to early spermatids; Table 1). Although only ~62% of the germ cells complete spermatogenesis in zebrafish, apoptotic germ cells are rarely detected in adult zebrafish.

Germ Cell and Leydig Cell Stereology and Cyst Volume

Although the total number of germ cells per cyst increased during spermatogenesis, the opposite was observed for the nuclear diameter and for the nuclear, cytoplasmic, and cellular volumes (Table 1). The trend was broken by a gradual but transient increase of these parameters in primary spermatocytes (from preleptotene to pachytene spermatocytes). Based on the

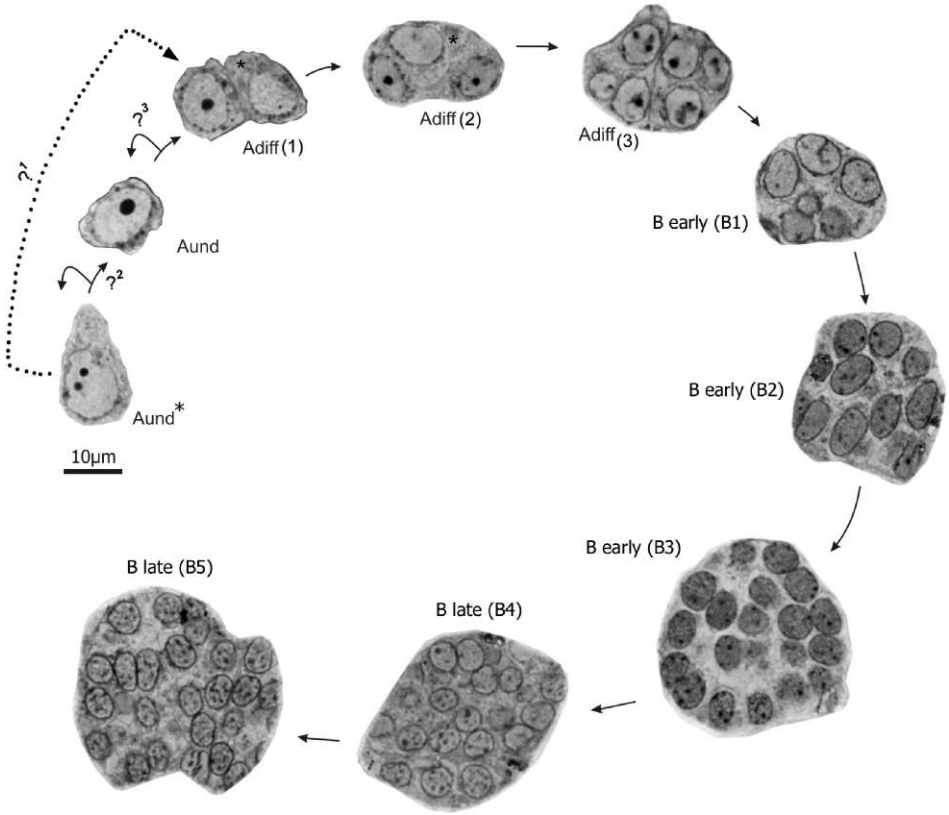

FIG. 3. Nine spermatogonial generations in zebrafish. The terminology addressing the different spermatogonial generations was based on morphological features, such as nuclear shape, heterochromatin amount, nucleolar characteristics, and number of germ cells in a cyst. Using high-resolution light microscopy applied to 1-μm-thick, araldite-embedded sections, we propose to differentiate five types of spermatogonia: type A undifferentiated* (A_{und}*; irregular outline of nuclear envelope and high ratio between cytoplasm and nucleus); type A undifferentiated (A_{und}; smooth outline of nuclear envelope and low ratio between cytoplasm and nucleus); type A differentiated (A_{diff} 1, 2, and 3), type B early (B1–B3), and type B late (B4 and B5). The first question mark ($?^1$) indicates a doubt regarding a possible asymmetric division of A_{und}* (dotted line leading to a pair of spermatogonia). The second question mark ($?^2$) indicates the doubt as to whether or not type A_{und}* is separated from type A_{und} by a mitosis. The third question mark ($?^3$) indicates uncertainty regarding the "stemness" of A_{und}. The asterisk inside the cells indicates spermatogonia showing the cytological charcateristics of type A_{und}* cells in small cysts with otherwise type A_{diff} spermatogonia, an observation possibly indicating asymmetrical division of A_{und}* (dotted line).

total number of germ cells per cyst and the individual volume of each germ cell type, we determined the total cyst volume, which showed a strong and steady increase from type A undifferentiated spermatogonium to pachytene spermatocytes, decreasing from this maximum to 85% in late spermatid cysts (Table 1).

The Leydig cell nuclear, cytoplasmic, and cell volumes were 53 ± 0.9 μm^3, 52 ± 0.7 μm^3, and 105 ± 1.6 μm^3, respectively. Leydig cells are not randomly distributed in the interstitial space but often form clusters, sometimes in the form of ringlike structures around blood vessels (Supplemental Fig. S2). Although not properly quantified, these clusters appeared to be larger in the periphery of the testis.

Spermatogonia Morphology, Spermatocytes, and Spermiogenesis

Two types of type A undifferentiated spermatogonia can be differentiated in zebrafish testes based on morphological criteria. They are referred to as type A undifferentiated* (A_{und}*) and type A undifferentiated (A_{und}; Fig. 3).

Both cell types differ from all later stages in that they are completely enveloped as a single cell by Sertoli cells and are the largest germ cells (~677 μm^3), with a large nucleus (diameter, 8.6 μm) containing poorly condensed chromatin and one or two compact nucleoli. Specific for type A_{und}* spermatogonia is that their nuclear envelope has an irregular outline that is not found in type A_{und} spermatogonia, and that the ratio between cytoplasm and nucleus is higher in type A_{und}* than in all other spermatogonia, including type A_{und} (Fig. 3).

The type A differentiated (A_{diff}) spermatogonia are very similar to the undifferentiated type. However, because these cells result from mitoses with incomplete cytokinesis, they are grouped (two, four, or eight) within the cyst and are smaller than the type A_{und} spermatogonia. The nucleus of type A_{diff} spermatogonia is denser and smaller, the nuclear envelope acquires a regular round shape, and two or three small nucleoli are found that assume eccentric positions (Fig. 3 and Supplemental Fig. S1). Moreover, heterochromatin starts to appear as flecks along the nuclear envelope (Fig. 3). When performing analysis by high-resolution light microscopy, we have sometimes observed small cysts of type A spermatogonia in which one of the germ cells showed morphological characteristics of type A_{und}* spermatogonia, and the other cells showed the characteristics of type A_{diff} spermatogonia (Fig. 3, asterisk in cysts with A_{diff}1 and A_{diff}2).

Type B early spermatogonia have an elongated/round nucleus with one or two small nucleoli. A major difference from type A spermatogonia is the increased amount of heterochromatin, which is distributed as round clumps throughout the nucleus or associated with the nuclear envelope (Fig. 3 and Supplemental Fig. S1).

In type B late spermatogonia, the number of germ cells inside the cyst increases (Table 1). The nucleus is round, smaller than in the early type B spermatogonia, and dense, and the heterochromatin (round clumps and associated with the nuclear envelope) reaches maximum density (Fig. 3 and Supplemental Fig. S1).

Spermatocytes in the different phases of meiosis can be identified by nuclear characteristics, such as size, chromosome condensation, and meiotic figures of the chromosomes (e.g., metaphase I or II; Fig. 2, G–K and Table 1). Leptotene/zygotene spermatocytes have a larger, rounder nucleus compared with the last generation of type B spermatogonia, showing a clear chromatin with small spots of heterochromatin bordering the nuclear envelope (Fig. 2H). Pachytene spermatocytes are the largest cell type among the spermatocytes. Their nucleus is denser and contains chromosomes as bold

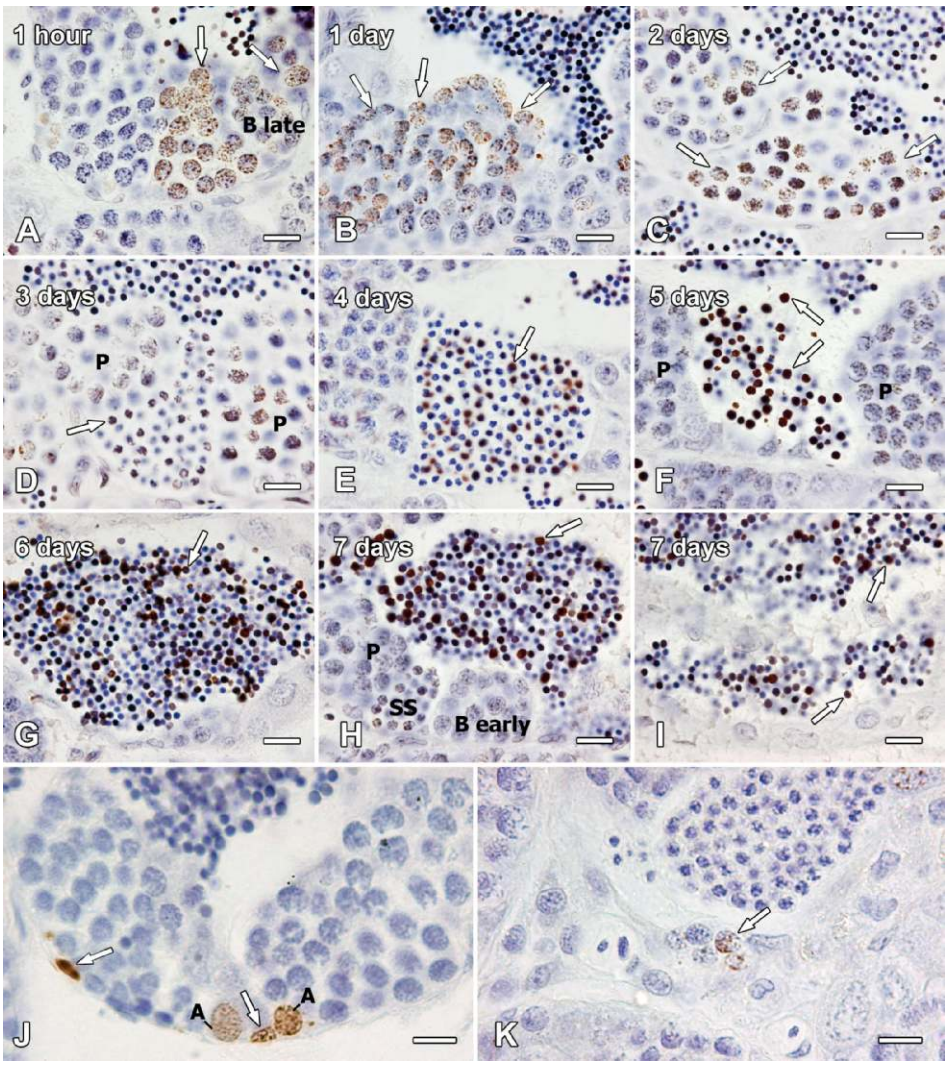

FIG. 4. Proliferating (BrdU-positive) somatic and germ cells in adult zebrafish testis. The following labeled cells were observed at different time periods after BrdU exposure: (**A**–**C**) at 1 h, and at 1 and 2 days, primary spermatocytes (pachytene, arrows); (**D** and **E**) at 3 and 4 days, spermatids (arrows); (**F**) at 5 days, spermatozoa (arrows) during spermiation; (**G** and **H**) at 6 and 7 days, spermatozoa (arrows) in the lumen of the seminiferous tubules; (**I**) at 7 days, spermatozoa (arrows) in the lumen of the efferent duct; (**J**) at 1 h, Sertoli (arrows); and (**K**) Leydig cell (arrow). A, type A spermatogonium; B early, early type B spermatogonia; B late, late type B spermatogonia; P, pachytene primary spermatocytes; SS, secondary spermatocytes. Bars = 10 μm (**A**–**I**) or 20 μm (**J** and **K**).

lines from the periphery to the central part of the nucleus (Fig. 2I). Diplotene spermatocytes are always found together with metaphasic figures (metaphase I; Fig. 2J). In this cell type, the chromosomes reach their maximum degree of condensation. Secondary spermatocytes are rare because they quickly enter into meiosis II. They have a round nucleus with a dense chromatin (Fig. 2K).

Spermiogenesis in zebrafish is marked by a striking reduction in the cellular volume (Table 1). We propose to differentiate three types of spermatids in zebrafish spermiogenesis: early (Fig. 2L), intermediate (Fig. 2M), and final spermatids (Fig. 2N). This classification is based on the increasing nuclear compaction and space between the spermatids (reflecting the loss of cytoplasmic bridges and the flagellum formation; Fig. 2, L–N).

Immunocytochemical and In Situ Hybridization Experiments

Our studies on molecular markers showed that antibodies against zebrafish Vasa and Piwil1 intensely labeled single type A undifferentiated spermatogonia and, in the case of Piwil1, also small cysts with type A differentiated spermatogonia (Supplemental Fig. S3, A and B). Vasa protein was also present at intermediate levels in differentiating spermatogonia and at low levels in spermatocytes, whereas spermatids and spermatozoa remained unlabeled. In the case of Piwil1, the labeling became very weak in late type B spermatogonia and spermatocytes, and it was not detected in haploid germ cells. The in situ hybridization for *pcna* mRNA, on the other hand, provided an intense labeling of more differentiated spermatogonia (Supplemental Fig. S3, C and D).

Duration of Spermatogenesis (Meiotic and Spermiogenic Phases)

The most advanced germ cells that carried a BrdU label after different periods following BrdU exposure at 27°C are shown in Figure 4. One hour after the termination of exposure (i.e., ~16 h after the start of contact with BrdU), the most advanced germ cells labeled were identified as early pachytene spermatocytes (Fig. 4A). At 1, 2, and 3 days after BrdU exposure, the most advanced cells labeled were late pachytene spermatocytes (Fig. 4, B–D), implying that it took less than 1 day to form pachytene from preleptotene spermatocytes. Four days after exposure, labeled spermatids were identified, whereas after 5 days we noticed the first labeled spermatozoa in the tubular lumen (Fig. 4, E and F). After 6 and 7 days of exposure, we regularly found labeled spermatozoa in the lumen of the seminiferous tubules (Fig. 4, G and H). Also, after 7 days, spermatozoa were found in the lumen of the efferent duct system (Fig. 4I). Based on these observations, we can estimate

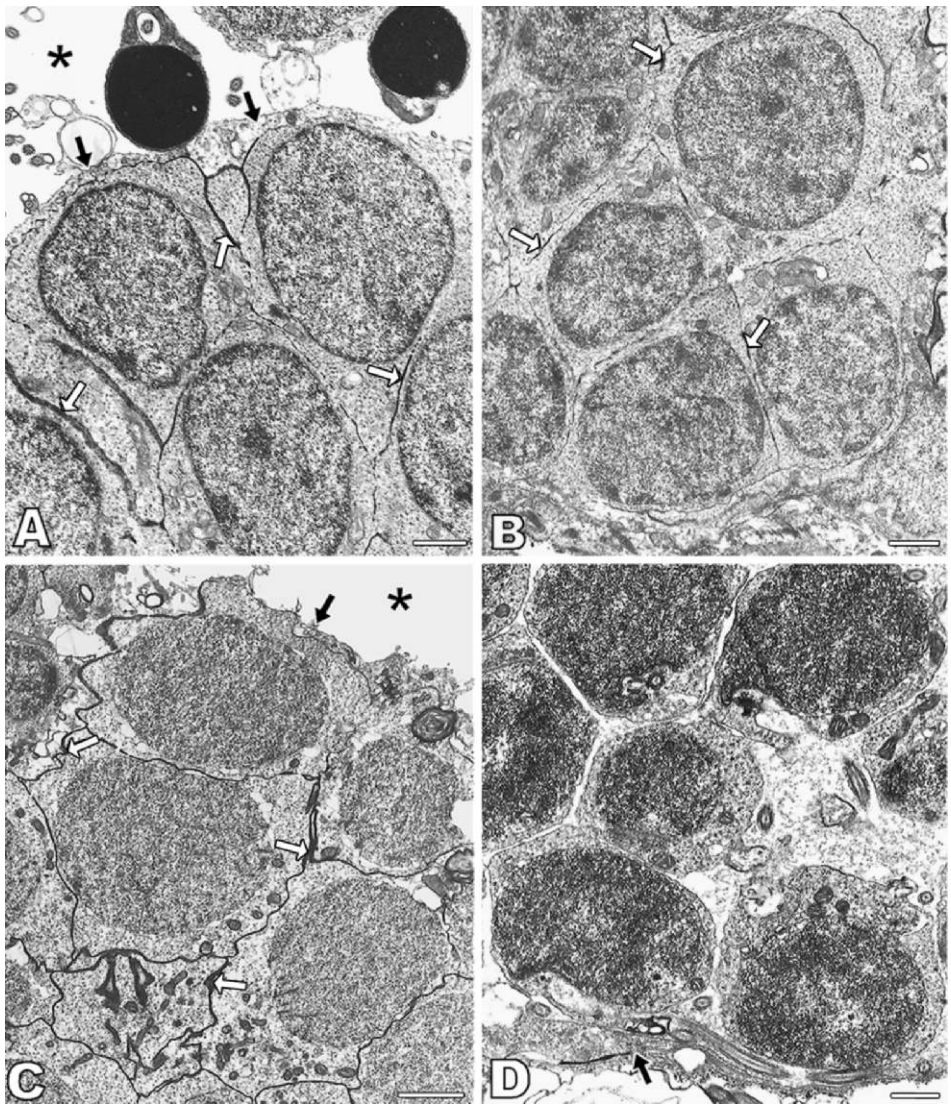

FIG. 5. Transmission electron microscopy of zebrafish testis sections using lanthanum as a tracer to investigate the permeability of the Sertoli cell barrier at different stages of spermatogenesis. The barrier is not observed in cysts containing type B spermatogonia (**A**) or primary spermatocyte cysts at the initial stages of meiosis (leptotene/zygotene; **B** and **C**), because lanthanum is present between the germ cells (white arrows). **D**) Lanthanum is found at the level of tight junctions between Sertoli cells in spermatid cysts (arrow). Note that the tracer is not present between the germ cells. The asterisks in the panels indicate the lumina of spermatogenic tubules, where lanthanum has never been found. The black arrows in **A** and **C** indicate the Sertoli cell cytoplasm. Bars = 1 μm (**A** and **B**), 2 μm (**C**), or 0.5 μm (**D**).

that the combined duration of meiotic and spermiogenic phases is very short in this species and lasts approximately 6 days (15 h of incubation plus 5 days after incubation).

Sertoli and Leydig cells were also labeled (Fig. 4, J and K), indicating that both cell types are able to proliferate in sexually mature animals.

Sertoli Cell Barrier

During spermatogenesis, lanthanum can be found inside spermatogonial and early meiotic cysts (leptotene/zygotene spermatocytes; Fig. 5, A and B). On the other hand, lanthanum was not found inside early spermatid cysts (Fig. 5, C and D), demonstrating that the Sertoli cell barrier (tight junctions) is established at the beginning of spermiogenesis, therefore obstructing the entry of lanthanum into the cyst lumen. Lanthanum has never been found in the lumen of spermatogenic tubules.

DISCUSSION

Testis Structure and Distribution of Spermatogonia

The zebrafish testicular parenchyma shows the typical vertebrate pattern with the germinal and interstitial compartments. As in other fishes and amphibians, the seminiferous tubules contain spermatogenic cysts formed by Sertoli cells that envelop a group of synchronously developing germ cells, which are derived in a clonal manner from one stem cell. The morphology of the different germ cell types observed for zebrafish is generally similar to what is described for most species of teleost fish [18, 19, 26–29], including the absence of acrosomes in spermatozoa [15].

Regarding the distribution of spermatogonia along the germinal compartment, two testis types have been described in fish: restricted and unrestricted [27–29]. In the restricted type (a derived character), undifferentiated type A spermatogonia are confined to the distal end of seminiferous tubules, near the tunica albuginea. In the unrestricted type (a primitive character), these spermatogonia are found at random sites along the seminiferous tubule throughout the testis. An intermediate type appears to exist in a number of orders (e.g., Gadiformes [30], Perciformes [18], Pleuronectiformes [31]), where undifferentiated type A spermatogonia show a preferential, but not exclusive, location close to the tunica albuginea. We have found that undifferentiated type A spermatogonia in zebrafish were distributed along the entire germinal compartment. The zebrafish testis belongs, therefore, to the unrestricted type. Moreover, zebrafish testes contain anastomosing tubules, which is another primitive feature

previously described in the orders Cypriniformes, Characiformes, Salmoniformes, and others [29].

Sertoli Cell Number

In the present study, the number of Sertoli cells per cyst was quantified using serial sections. The final number of Sertoli cells in mammals is established at puberty, when Sertoli cells cease proliferating and differentiate terminally [6]. Because a Sertoli cell's capacity to support germ cells is limited, Sertoli cell number limits testis size and determines the spermatogenic capacity [32]. Data on the Sertoli cell number for teleosts with external fertilization are only available for *Oreochromis niloticus* [18–20] and zebrafish (this study). In both species, the number of Sertoli cells per cyst increased (4-fold in tilapia, 9-fold in zebrafish) and tended to stabilize in the meiotic phase, attaining a ratio of ~92 and ~95 spermatids per Sertoli cell in tilapia and zebrafish, respectively. During spermatogenesis in guppies (*Poecilia reticulata*), a species with internal fertilization, it was observed that the number of Sertoli cells per cyst also increased considerably (~30-fold, from ~4 to ~130 Sertoli cells per cyst) from a cyst with a single, undifferentiated spermatogonium until the initial phase of the spermiogenesis, when nearly 24 000 spermatids per cyst were found (i.e., ~170 spermatids per Sertoli cell [33]). We conclude that it is a typical feature of adult teleost spermatogenesis that Sertoli cell number increases per cyst during its development. Detailed studies in tilapia and African catfish [18, 19] showed that the vast majority of dividing (i.e., incorporating ^{3}H-thymidine or BrdU) Sertoli cells were associated with expanding spermatogonial cysts. It may not seem surprising, therefore, that we have found proliferating Sertoli cells in the testes of young adult zebrafish. However, tilapia and catfish show life-long somatic and testis growth, unlike birds or mammals and unlike zebrafish. However, a certain growth of both body and testis takes place after the zebrafish have completed puberty (first reproduction) at approximately 12 wk of age. At this point, we are unable to determine whether the observed Sertoli cell proliferation represents remaining growth until attainment of final testis size, or whether during cystic spermatogenesis a certain loss of Sertoli cells occurs that requires compensatory proliferation. The scarce literature available on Sertoli cells in teleosts speculates that after spermiation, these cells can degenerate or become integrated into the epithelium of the spermatic ducts [10, 28, 34]. Similar to what was observed in tilapia [18, 19], and despite analyzing several hundreds of cysts in zebrafish, Sertoli cells with the morphological characteristics of apoptosis were not observed. One explanation may be that the very high phagocytotic activity of Sertoli cells [35] removes apoptotic Sertoli cells quickly, so that they do not accumulate to a noticeable degree. Alternatively, Sertoli cells may be "recycled" after spermiation to contribute to the formation/growth of a new/still developing cyst.

Sertoli Cell Efficiency and Germ Cell Loss

Considering the number of spermatids per Sertoli cell in zebrafish, tilapia, and guppies (90–170) [18–20, 33], the Sertoli cell efficiency is quite high in fish, with their cystic arrangement of the spermatogenic process—10 to 20 times higher than in mammals [6, 36, 37]. Despite the great range in the number of spermatids per cyst in tilapia, zebrafish, and guppies (~650, ~1300, and ~24 000, respectively), the efficiency of the Sertoli cells in these three species of teleost fish is relatively similar. Moreover, experimentally induced changes in Sertoli cell numbers led to corresponding changes in germ cell numbers in tilapia [20], suggesting that, like in mammals [37], the number of Sertoli cells is the main factor determining the magnitude of the sperm production.

Germ cell apoptosis constitutes a normal process during spermatogenesis [38] and can occur in different developmental phases. In mammals, it is considered mainly to function in density regulation of spermatogonia and to eliminate cells with chromosomal damage (meiotic phase), whereas cell loss during spermiogenesis is less prominent [37]. The quantitative significance of germ cell loss becomes clear when considering that in mammals, only two to three spermatozoa of 10 theoretically possible cells are produced from type A1 spermatogonia [7, 37]. In the present study, we found that instead of the theoretically expected 2048 mature spermatids, approximately 1300 were formed. Hence, 6 of 10 possible cells reached the final stages of development, which contributes to the high efficiency of fish spermatogenesis. We speculate that the tailored proliferation of Sertoli cells is a relevant factor for the high survival rate of germ cells in the fish testis.

Apoptosis is mainly found during spermiogenesis in tilapia (~25% vs. ~10%), whereas in zebrafish there is a greater loss (~20% vs. 10%) during the spermatogonial phase. In both species, about 10% apoptosis occurred during meiosis. In guppies [33] and Atlantic cod [30], the main loss of germ cells occurred in the spermatogonial phase. These findings suggest that although the total losses are quite similar among fish species, apoptosis can occur during different stages along the spermatogenic process, which may reflect differences in the fine regulation of this process. The frequency with which apoptotic cells were observed in sections was surprisingly low, despite the overall loss of ~40% of germ cells. We ascribe this apparent discrepancy to the high phagocytotic efficiency of zebrafish Sertoli cells [35]. However, our understanding of the process of apoptosis and its regulation in fish is still incipient, and only a few species of teleost fish have been investigated in this regard.

Spermatogonial Generations

Knowing the precise number of spermatogonial divisions is fundamental to understanding the regulation of spermatogenesis. Previous reports stated that the number of spermatogonial generations in teleosts varies from four to six in zebrafish [39, 40] up to 14 in guppy [33], and intermediate values are observed in other teleost species [18, 26, 40]. Stereological analysis of spermatogenic cysts, as done by serial sections in the present study, is a laborious but powerful approach to establish the number of cells per cyst, which allows deduction of the number of spermatogonial generations. This permitted the calculation that nine generations of spermatogonia (type A undifferentiated spermatogonia, three generations of type A differentiating spermatogonia, and five generations of type B spermatogonia) are present in zebrafish. Ando and collaborators [40] reported four or five generations of spermatogonia in zebrafish, but the conclusion was based on counting spermatids in single sections where the cysts showed the maximum diameter. The difference in results may be based on the fact that this approach assumes a spherical shape of spermatid cysts and would lead to an underestimation of cell numbers if the actual shape was irregular or elongated, which is not unusual in zebrafish according to our observations.

Spermatogonial morphology in fish has been described on the light [19, 28, 30, 31, 33, 41, 42] and electron [41–43] microscopy levels. However, there is no consensus about the terminology used to address the different spermatogonial generations in this group of vertebrates. This difficulty is in part due to the cystic mode of spermatogenesis, so that—unlike

the situation in reptiles, birds, and mammals—there are no stages (specific cellular associations) in the seminiferous epithelium of fish. Two types of spermatogonia have been described in fish considering basically the size and number of cells within the cysts. For example, single, larger spermatogonia were designated primary spermatogonia or type A spermatogonia; smaller and grouped spermatogonia (in pairs or more), on the other hand, were referred to as secondary or type B spermatogonia [44, 45]. However, close morphofunctional analysis reveals cells with significant differences in morphology and kinetics among the secondary or type B spermatogonia, with some generations being more similar to the type A undifferentiated spermatogonia and others more similar to the more differentiated types of smaller spermatogonia in medium-sized or large groups. Hence, the first generations of grouped spermatogonia in small cysts share a number of characteristics with the single spermatogonia in fish as well as with the type A spermatogonia in rodents. Therefore, based on similar criteria (e.g., nuclear and nucleolar features, and the presence, amount, and distribution of heterochromatin) used to discriminate between different types of spermatogonia in rodents [46], we evaluated zebrafish testes with high-resolution light microscopy and proposed a nomenclature for spermatogonial generations that is in line with established systems in higher vertebrates. In this way, we have described the following sequence of spermatogonial generations: undifferentiated type A spermatogonia (A_{und}* and A_{und}) → type A differentiated (A_{diff}) → type B early (B_{early}) → type B late (B_{late}). A_{und}* and A_{und} are single cells with a large nucleus containing poorly condensed chromatin and one or two nucleoli. A_{und}* spermatogonia have an irregular nuclear envelope that is not found in type A_{und}. A_{diff} are grouped (approximately two, four, or eight) within the cyst, and their nucleus is denser than in the previous spermatogonial generation, with heterochromatin as flecks along the nuclear envelope. The type B early spermatogonia (theoretically 16–32 cells; we counted 14–28 cells) have an elongated/round nucleus with one or two small nucleoli. A major difference from type A spermatogonia is the increased amount of heterochromatin that is distributed as round clumps throughout the nucleus or associated with the nuclear envelope. In the type B late spermatogonia (~55 to 208 cells), the nucleus is round, smaller, and more dense, and the heterochromatin forms round clumps associated with the nuclear envelope.

This morphological classification is standardized and reproducible for the zebrafish, and it can be applied to other fish species as well, except perhaps for the absolute values of the cell/nuclear sizes, whereas the relative changes of these parameters are found also in other species [20, 33]. Therefore, this categorization may provide a basis for standardizing the nomenclature used for spermatogonia in fish. Moreover, this classification parallels the nomenclature in mammals, mainly regarding the amount of heterochromatin, which is expected to simplify comparative approaches. Especially in mice, this approach has been used extensively [46, 47]. Finally, the present classification has the flexibility to allow for adjustments if required by future results—for example, regarding the molecular and/or functional characterization of the different developmental stages of germ cells, such as indicated by the expression analysis of stage-specific proteins/mRNAs (Supplemental Fig. S3) or by the capacity of germ cells to colonize a recipient's testis after transplantation (stemness) [48, 49].

The coexistence of undifferentiated and differentiated spermatogonia type A in the same cyst is intriguing in the context of stemness of spermatogonia. We were able to make this observation because the high-resolution approach allowed identifying cell membranes and cyst borders on the light microscopy level. Future work will have to evaluate the ratio of equal:unequal division of type A_{und}* spermatogonia (e.g., stem cell self-renewal vs. differentiation fate) and the regulation of this balance—for instance, regarding the orientation of the mitotic spindle pole, such as that described in *Drosophila* testis [50], or regarding factors (e.g., glial cell line-derived neurotrophic factor) secreted by Sertoli cells in rodents (see De Rooij [51] for review). In addition, an intriguing question to be investigated in fish refers to the "stemness" of a subset of differentiating spermatogonia, as has been described recently for mouse testis under certain injury conditions [52].

Meiotic and Postmeiotic Cells

Compared with the studies on tilapia [18, 19], where the same methods were used as here, the size of germ cells in zebrafish is ~3-fold smaller in practically all of the spermatogenic phases, notwithstanding that a similar pattern was found regarding the morphological changes during spermatogenesis in zebrafish, tilapia, and guppies [33]. A noticeable exception in guppies is that the maximum diameter among primary spermatocytes was observed in zygotene cells.

In general, volume changes of meiotic and postmeiotic germ cells in zebrafish and tilapia were similar to those observed in mammals [37]. However, in mammals, diplotene spermatocytes show the maximum volume [37]. We do not have an explanation for the shift to pachytene in teleosts (zygotene in guppies) at present. It seems reasonable to expect the maximum cell volume in diplotene spermatocytes that have accumulated the genetic and cytoplasmic material required for the two upcoming fast meiotic divisions and the formation of spermatids [37]. Clearly, this aspect of teleost spermatogenesis deserves further study. With pachytene spermatocytes being the biggest cell type in the meiotic phase, it is not surprising that pachytene cysts also show the maximum average volume of spermatogenic cysts. Cyst volume decreased progressively during spermiogenesis. This may reflect the remarkable nuclear condensation and elimination of cell organelles and cytoplasm during spermiogenesis [18, 19, 37, 53, 54]. Moreover, apoptotic loss of germ cells also occurs during this stage (see above).

Leydig Cells

We are not aware of studies on the individual volume of Leydig cells in teleosts other than tilapia [20, 48]. Similarly to the germ cells, Leydig cells in tilapia were 3- to 4-fold larger than observed here in zebrafish. In mammals, Leydig cell volume can vary from ~400 μm^3 in ovine and wild boars [55, 56] to ~5000 μm^3 in horses [57], with most species ranging between 1000 and 2000 μm^3 [56, 58]. Hence, the volume of Leydig cell ranges at the low end of this comparative scale. As in other fish [12], Leydig cells formed groups or clusters with extensive plasma membrane contact zones. Although we did not quantify this aspect, it seems that Leydig cell clusters were larger/contained more cells close to the tunica albuginea than in central areas of the testis.

Duration of Spermatogenesis (Meiotic and Spermiogenic Phases)

A number of studies have dealt with the duration of spermatogenesis in teleosts [18, 39, 59–63]. Determining the duration of spermatogenesis in mammals is classically based on the fact that the different germ cell generations form specific, recurrent cell associations, known as stages of the seminiferous epithelium. The determination of their relative frequencies

enables the total duration of the differentiation process from stem cells to spermatozoa to be deduced [6, 37, 56, 58, 64]. In cystic spermatogenesis, however, this approach is not feasible. It is possible, however, to determine the duration of the meiotic and spermiogenic phases (i.e., from preleptotene/leptotene up to spermatozoa). This period is identical to the time required for an S-phase marker, such as BrdU, which is incorporated during the final round of DNA synthesis, to appear in spermatozoa. Using this approach, we found that the combined duration of the meiotic and spermiogenic phases is about 6 days in zebrafish. This is similar to the duration found in an Indian freshwater perch, *Colisa fasciata* [65], whereas a period of 3 wk was the longest found among teleosts in black mollies *Poecilia sphenops* [61]. In general, fish germ cells proceed faster through meiosis/spermiogenesis than mammalian germ cells, which take 3–7 wk [37, 56].

Different from the homoeothermic mammals, the duration of spermatogenesis in fish varies depending on the water/body temperature [66]. Studies describing the effects of temperature on the duration of spermatogenesis in fish [59, 60] or reptiles [67] showed that in general, elevated temperatures accelerate germ cell development. The fact that zebrafish usually reproduce in temperatures close to 30°C can explain, at least in part, the short duration of the meiotic and spermiogenic phases. The short duration, a high number of spermatogonial generations, and a high efficiency of the Sertoli cell jointly allow the prediction that the daily sperm production per volume unit of the zebrafish testicular parenchyma will be rather high.

Sertoli Cell Barrier

Experimental evidence of the Sertoli cell barrier ("blood-testis barrier") became available when certain dyes were incapable of reaching meiotic and postmeiotic germ cells in the mammalian seminiferous epithelium [68, 69]. The use of electron-dense tracers, such as lanthanum, showed in mice [70, 71] that tight junctions between neighboring Sertoli cells in the seminiferous epithelium prevented the passage of the tracer. The Sertoli cell barrier has been demonstrated in all other classes of vertebrates (birds [72], reptiles [73], amphibians [74], and fish [75, 76]). It appears that the effective seclusion of the genetically and immunologically distinct meiotic and postmeiotic cells is an important, evolutionarily conserved principle in spermatogenesis.

In fish, depending on the species, the establishment of the tight junctions between Sertoli cells occurs in cysts containing primary spermatocytes [75] or spermatids [12, 77, 78]. In zebrafish, lanthanum was detected among spermatogenic cells until the beginning of the meiotic prophase but was excluded from cysts containing early spermatids, demonstrating that the Sertoli cell barrier is established at the end of meiotic phase. Interestingly, we have never observed lanthanum in the lumen of spermatogenic tubules, even though it was able to enter cycts containing germ cells up to the stage of leptotene/zygotene spermatocytes. Therefore, we consider it possible that future analysis will provide evidence for tight junctions among adluminal Sertoli cells (i.e., separating the lumen of spermatogenic tubules from the lumen of spermatogenic cysts) already being established shortly after cyst formation. The formation of tight junctions among Sertoli cells at the basal part of the germinal epithelium, on the other hand, appears to depend on the stage of development of the germ cells. This situation suggests that not only in mammals but also in zebrafish, the germinal epithelium is polarized. Regarding the establishment of the microenvironment required for germ cell development, other structures besides the Sertoli cell barrier may be involved, such as the capillary endothelium, the basal lamina, and peritubular myoid cells [78].

In conclusion, this is the first detailed study using morphological, stereological, and molecular approaches on spermatogenesis in zebrafish. Also, we are proposing a new nomenclature for the spermatogonial generations in zebrafish that will allow further comparisons with other fishes but also with higher vertebrates, such as mammals. The new results obtained for the zebrafish in the present study contribute to the characterization of the testicular function in this important teleost model species, which may be of great value in future studies on the regulation of spermatogenesis.

ACKNOWLEDGMENTS

The authors would like to thank R.F. Ketting and S. Houwing (Hubrecht Laboratory, Utrecht, The Netherlands) for providing the antibody against zebrafish Piwil1.

REFERENCES

1. Engeszer RE, Patterson LB, Rao AA, Parichy DM. Zebrafish in the wild: a review of natural history and new notes from the field. Zebrafish 2007; 4: 21–40.
2. McGonnell IM, Fowkes RC. Fishing for gene function–endocrine modeling in the zebrafish. J Endocrinol 2006; 189:425–439.
3. Briggs JP. The zebrafish: a new model organism for integrative physiology. Am J Physiol Regul Integr Comp Physiol 2002; 282:R3–R9.
4. Aleström P, Holter JL, Nourizadeh-Lillabadi R. Zebrafish in functional genomics and aquatic biomedicine. Trends Biotechnol 2006; 24:15–21.
5. Dahm R, Geisler R. Learning from small fry: the zebrafish as a genetic model organism for aquaculture fish species. Mar Biotechnol (NY) 2006; 8:329–345.
6. Hess RA, França LR. Structure of the Sertoli cell. In: Skinner MK, Griswold MD (eds.), Sertoli Cell Biology. San Diego, CA: Elsevier Academic Press; 2005:19–40.
7. De Rooij DG, Russell LD. All you wanted to know about spermatogonia but were afraid to ask. J Androl 2000; 21:776–798.
8. De Rooij DG. Regulation of spermatogonial stem cell behavior in vivo and in vitro. Anim Reprod 2006; 3:130–134.
9. Ehmcke J, Wistuba J, Schlatt S. Spermatogonial stem cells: questions, models and perspectives. Hum Reprod Update 2006; 12:275–282.
10. Pudney J. Comparative cytology of the non-mammalian vertebrate Sertoli cell. In: Russell LD, Griswold MD (eds.), The Sertoli Cell. Clearwater, FL: Cache River Press; 1993:612–657.
11. Pudney J. Comparative cytology of the Leydig cell. In: Payne AH, Hardy MP, Russell LD (eds.), The Leydig Cell. Vienna, IL: Cache River Press; 1996:98–142.
12. Loir M, Sourdaine P, Mendis-Handagama SM, Jégou B. Cell-cell interactions in the testis of teleost and elasmobranchs. Micr Res Tech 1995; 32:533–552.
13. Jones RC, Lin M. Spermatogenesis in birds. Oxf Rev Reprod Biol 1993; 15:233–264.
14. Gribbins KM, Elsey RM, Gist DH. Cytological evaluation of the germ cell development strategy within the testis of the American alligator, *Alligator mississippiensis*. Acta Zool (Stockholm) 2006; 87:59–69.
15. Nóbrega RH, Batlouni SR, França LR. An overview of functional and stereological evaluation of spermatogenesis and germ cell transplantation in fish. Fish Physiol Biochem 2009; 35:197–206.
16. Nash JP, Kime DE, Van der Ven LT, Wester PW, Brion F, Maack G, Stahlschmidt-Allner P, Tyler CR. Long-term exposure to environmental concentrations of the pharmaceutical ethynylestradiol causes reproductive failure in fish. Environ Health Perspect 2004; 112:1725–1733.
17. Van den Hurk R, Schoonen WG, van Zoelen GA, Lambert JG. The biosynthesis of steroid glucuronides in the testis of the zebrafish, *Brachydanio rerio*, and their pheromonal function as ovulation inducers. Gen Comp Endocrinol 1987; 68:179–188.
18. Vilela DAR, Silva SGB, Peixoto MTD, Godinho HP, França LR. Spermatogenesis in teleost: insights from the Nile tilapia (*Oreochromis niloticus*) model. Fish Physiol Biochem 2003; 28:187–190.
19. Schulz RW, Menting S, Bogerd J, França LR, Vilela DAR, Godinho HP. Sertoli cell proliferation in the adult testis–evidence from two fish species belonging to different orders. Biol Reprod 2005; 73:891–898.
20. Matta SLP, Vilela DAR, Godinho HP, França LR. The goitrogen 6-n-propyl-2-thiouracil (PTU) given during testis development increases

Sertoli and germ cell numbers per cyst in fish: the tilapia (*Oreochromis niloticus*) model. Endocrinology 2002; 143:970–978.
21. Braat AK, van de Water S, Goos H, Bogerd J, Zivkovic D. Vasa protein expression and localization in the zebrafish. Mech Dev 2000; 95:271–274.
22. Houwing S, Kamminga LM, Berezikov E, Cronembold D, Girard A, van den Elst H, Filippov DV, Blaser H, Raz E, Moens CB, Plasterk RH, Hannon GJ, et al. A role for Piwi and piRNAs in germ cell maintenance and transposon silencing in zebrafish. Cell 2007; 129:69–82.
23. Essers J, Theil AF, Baldeyron C, van Cappellen WA, Houtsmuller AB, Kanaar R, Vermeulen W. Nuclear dynamics of PCNA in DNA replication and repair. Mol Cell Biol 2005; 25:9350–9359.
24. Miura C, Miura T, Yamashita M. PCNA protein expression during spermatogenesis of the Japanese eel (*Anguilla japonica*). Zool Sci 2002; 19:87–91.
25. Van de Kant HJG, de Rooij DG. Periodic acid incubation can replace hydrochloric acid hydrolysis and trypsin digestion in immunogold-silver staining of bromodeoxyuridine incorporation in plastic sections and allows the PAS reaction. Histochem J 1992; 24:170–175.
26. Miura T. Spermatogenic cycle in fish. In: Knobil E, Neill JD (eds.), Encyclopedia of Reproduction. San Diego: Academic Press; 1999: 4:571–578.
27. Grier HJ, Linton JR, Leatherland JF, De Vlaming VL. Structural evidence for two different testicular types in teleost fishes. Am J Anat 1980; 159: 331–345.
28. Grier HJ. Cellular organization of the testis and spermatogenesis in fishes. Am Zool 1981; 21:345–357.
29. Parenti LR, Grier HJ. Evolution and phylogeny of gonad morphology in bony fishes. Integr Comp Biol 2004; 44:333–348.
30. Almeida FFL, Kristoffersen C, Taranger GL, Schulz RW. Spermatogenesis in Atlantic cod (*Gadus morhua*): a novel model of cystic germ cell development. Biol Reprod 2008; 78:27–34.
31. Garcia-Lopez A, Martinez-Rodriguez G, Sarasquete C. Male reproductive system in Senegalese sole *Solea senegalensis* (Kaup): anatomy, histology and histochemistry. Histol Histopathol 2005; 20:1179–1189.
32. Petersen C, Soder O. The Sertoli cell–a hormonal target and 'super' nurse for germ cells that determines testicular size. Horm Res 2006; 66:153–161.
33. Billard R. La spermatogenèse de *Poecilia reticulata*. I–estimation du nombre de générations goniales et rendement de la spermatogenèse. Ann Biol Anim Biochim Biophys 1969; 9:251–271.
34. Van den Hurk R, Peute J, Vermeij JAJ. Ultrastructural study of the testis of the black molly (*Mollienisia latipinna*) I. The intratesticular efferent duct system. Proc Kon Ned Akad Wet Ser 1974; 77:460–469.
35. Leal MC, Feitsma H, Cuppen E, França LR, Schulz RW. Completion of meiosis in male zebrafish (*Danio rerio*) despite lack of DNA mismatch repair gene *mlh1*. Cell Tissue Res 2008; 332:133–139.
36. Sharpe RM. Regulation of spermatogenesis. In: Knobil E, Neill JD (eds.), The Physiology of Reproduction. New York: Raven Press; 1994:1363–1434.
37. França LR, Russell LD. The testis of domestic animals. In: Martínez-García F, Regadera J (eds.), Male Reproduction: A Multidisciplinary Overview. Madrid: Churchill Communications; 1998:198–219.
38. Baum JS, St George JP, McCall K. Programmed cell death in the germ line. Semin Cell Dev Biol 2005; 16:245–259.
39. Ewing HH. Spermatogenesis in the zebrafish, *Brachydanio rerio*. Anat Rec 1972; 172:308.
40. Ando N, Miura T, Nader MR, Miura C, Yamauchi K. A method for estimating the number of mitotic divisions in fish testes. Fisheries Sci 2000; 66:299–303.
41. Billard R. A quantitative analysis of spermatogenesis in the trout, *Salmo trutta fario*. Cell Tiss Res 1983; 230:495–502.
42. Lo Nostro FL, Grier H, Meijide FJ, Guerrero GA. Ultrastructure of the testis in *Synbranchus marmoratus* (Teleostei, Synbranchidae): the germinal compartment. Tissue Cell 2003; 35:121–132.
43. Quagio-Grassiotto I, Carvalho ED. The ultrastructure of *Sorubim lima* (Teleostei, Siluriformes, Pimelodidae) spermatogenesis: premeiotic and meiotic periods. Tissue Cell 1999; 31:561–567.
44. Billard R. Ultrastructural changes in the spermatogonia and spermatocytes of *Poecilia reticulata* during spermatogenesis. Cell Tissue Res 1984; 237: 219–226.
45. Selman K, Wallace RA. Gametogenesis in *Fundulus heteroclitus*. Am Zool 1986; 26:173–192.
46. Chiarini-Garcia H, Meistrich ML. High-resolution light microscopic characterization of spermatogonia. In: Hou SX, Singh SR (eds.), Germline Stem Cells. Methods in Molecular Biology. Totowa, NJ: Humana Press, Springer Science; 2008; 450:95–107.
47. Chiarini-Garcia H, Russell LD. Characterization of mouse spermatogonia by transmission electron microscopy. Reproduction 2002; 123:567–577.
48. Lacerda SMSN, Batlouni SR, Silva SBG, Homem CSP, França LR. Germ cells transplantation in fish: the Nile-tilapia model. Anim Reprod 2006; 3: 146–159.
49. Shikina S, Ihara S, Yoshizaki G. Culture conditions for maintaining the survival and mitotic activity of rainbow trout transplantable type A spermatogonia. Mol Reprod Dev 2008; 75:529–537.
50. Fuller MT, Spradling AC. Male and female *Drosophila* germline stem cells: two versions of immortality. Science 2007; 316:402–404.
51. De Rooij DG. Proliferation and differentiation of spermatogonial stem cells. Reproduction 2001; 121:347–354.
52. Nakagawa T, Nabeshima Y, Yoshida S. Functional identification of the actual and potential stem cell compartments in mouse spermatogenesis. Dev Cell 2007; 2:195–206.
53. Grier HJ. Sperm development in the teleost *Oryzias latipes*. Cell Tissue Res 1976; 168:419–431.
54. Sprando RL, Heidinger RC, Russell LD. Spermiogenesis in the bluegill (*Lepomis macrochirus*): a study of cytoplasmic events including cell volume changes and citoplasmic elimination. J Morphol 1988; 198:165–177.
55. Lunstra DD, Schanbacher BD. Testicular function and Leydig cell ultraestructure in long-term bilateral cryptorchid rams. Biol Reprod 1988; 38:211–220.
56. Almeida FFL, Leal MC, França LR. Testis morphometry, duration of spermatogenesis and spermatogenic efficiency in the wild boar (*Sus scrofa scrofa*). Biol Reprod 2006; 75:792–799.
57. Johnson L, Neaves WB. Age related changes in the Leydig cell population, seminiferous tubules and sperm population in stallions. Biol Reprod 1981; 24:703–712.
58. Leal MC, França LR. The seminiferous epithelium cycle length in the black tufted-ear marmoset (*Callithrix penicillata*) is similar to humans. Biol Reprod 2006; 74:616–624.
59. Egami N, Hyodo-Taguchi Y. An autoradiographic examination of rate of spermatogenesis at different temperatures in the fish, *Oryzias latipes*. Exp Cell Res 1967; 47:665–667.
60. Billard R. Influence de la température sur la durée et l'efficacé de la spermatogenèse du guppy, *Poecilia reticulata*. C R Acad (Paris) 1968; 206:2287–2290.
61. De Felice DA, Rasch EM. Chronology of spermatogenesis and spermiogenesis in Poeciliid fishes. J Exp Zool 1969; 171:191–208.
62. Silva M, Godinho HP. Timing of some events of the gametogenesis in the male Nile tilapia, *Sarotherodon niloticus*. Arch Anat Microsc Morphol Exp 1983; 72:231–237.
63. Sinha GM, Mondal SK, Ghosal SK. Meiosis and spermiogenesis in a freshwater teleost fish, *Channa punctatus* (Bloch): an estimation of their duration by autoradiographic method. Cytol 1983; 48:87–93.
64. França LR, Ogawa T, Avarbock MR, Brinster RL, Russell LD. Germ cell genotype controls cell cycle during spermatogenesis in the rat. Biol Reprod 1998; 59:1371–1377.
65. Sinha GM, Mondal SK, Midya T, Ghosal SK. Chronology of meiosis and spermiogenesis in a fresh-water teleost fish, *Colisa fasciata* (Bloch and Schneider). Z Mikrosk Anat Forsch 1979; 93:442–448.
66. Billard R. Spermatogenesis and spermatology of some teleost fish species. Reprod Nutr Dev 1986; 26:877–920.
67. Licht P, Basu SL. Influence of temperature on lizard testes. Nature 1967; 213:672–674.
68. Setchell BP. The blood-testicular fluid barrier in sheep. J Physiol 1967; 189:63–65.
69. Dym M, Fawcett DW. The blood-testis barrier in the rat and the physiological compartimentation of the seminiferous epithelium. Biol Reprod 1970; 3:308–326.
70. Fawcett DW, Leak LV, Heidger PM Jr. Electron microscopic observations on the structural components of the blood-testis barrier. J Reprod Fertil Suppl 1970; 10:105–122.
71. Ross MH. Sertoli-Sertoli junctions and Sertoli-spermatid junctions after efferent ductule ligation and lanthanum treatment. Am J Anat 1977; 148:49–55.
72. Bergmann M, Schindelmeiser J. Development of the blood testis barrier in the domestic fowl (*Gallus domesticus*). Int J Androl 1987; 10:482–488.
73. Baccetti B, Bigliardi E, Vegni Talluri M, Burrini AG. The Sertoli cell in lizards. J Ultrastruct Res 1983; 85:11–23.
74. Franchi E, Camatini M, de Curtis I. Morphological evidence of a permeability barrier in urodele testis. J Ultrastruct Res 1982; 80:253–263.
75. Abraham M, Rahamim E, Tibika H, Golenser E, Kieselskin M. The blood-testis barrier in *Aphanius dispar* (Teleostei). Cell Tissue Res 1980; 211: 207–214.
76. Silva S, Godinho HP. Barreira hemotesticular em *Oreochromis niloticus* (peixe-teleósteo). Rev Bras Ciênc Morfol 1989; 6:9–13.
77. Billard R. La spermatogenèse de *Poecilia reticulata* III. Ultrastructure des cellules de Sertoli. Ann Biol Anim Biochim Biophys 1970; 10:37–50.
78. Abraham M. The male germ cell protective barrier along phylogenesis. Int Rev Cytol 1991; 130:111–190.